Analysis of Point Cloud Generation from UAS Images

[redacted]

[redacted]

ISPRS TC I Symposium 2014

KEY WORDS: UAV, UAS, Point Cloud, Block Triangulation, Software Comparison

ABSTRACT:

Unmanned Aerial Systems (UAS) allow for the collection of low altitude aerial images, along with other geospatial information from a variety of sensors able to be attached. The images can then be processed using sophisticated techniques from the Computer Vision (CV) field, along with traditional procedures from photogrammetry. Based on highly overlapped images, new software packages which were specifically developed for UAS technology can easily create ground models such as Point Clouds (PC), Digital Surface Model (DSM), orthoimages, etc. The goal of this study is to compare the performance of three different software packages, including the accuracy of the 3D products they produce. Using an ocotocopter UAS platform with a Nikon D800 camera, images were collected during two field tests conducted over the Olentangy River, north from the [redacted] campus. Both were focused over bike bridges on the Olentangy River Trail. These sites were selected because of the challenge the packages would have in creating accurate products; matching pixels over the river and dense canopy on the shore presents difficult scenarios to model. Ground Control Points (GCP) were gathered at each site to tie the models to a local coordinate system and help assess the absolute accuracy for each package. The models created by each package were also relatively compared to each other using their PCs.

1. INTRODUCTION AND BACKGROUND

The [redacted] Lab has been involved in research using the low cost and widely accessible UAS technology. The goal of the research is to exploit the technology using an octocopter UAS platform, with a variety of sensor configurations, including: optical cameras, GPS receivers, laser scanners, inertial measurement units (IMU), etc., to create accurate survey and engineering grade ground models as well as positioning data. The integration of different sensors and technologies into this UAS system is vital in gathering the most accurate data, and subsequently, creating high quality geospatial products.

As with any emerging technology, both hardware and software components are relatively new and still rapidly developing, thus the reliability and efficiency continues to improve. The possibilities of UAS data are practically limitless, including accurate positioning and object space modeling for uses as different as defense special operation applications to archaeological and environmental studies applications (Haubeck, 2013; Niethammer, 2011).

There are two approaches to utilizing image data from UAS technology to create 3D models and spatial data. The first is with traditional photogrammetry where the images are aerial triangulated (AT) to obtain sensor orientation, also referred to as indirect georeferencing (Mikhail, 2001). Then, the actual model creation is performed, which could be manual or semi-automatic. This approach generally produces highly accurate 3D position and orientation and is usually based on integrated sensor orientation (ISO). Note that sensor self-calibration is also available. The second approach is based on dense matching (pixel level), and uses bundle block adjustment (Gini, 2013). This is also a variant of indirect georeferencing, as GCPs are used to generate 3D ground coordinates for a model. Note that it allows for model creation without the exact camera locations, though, it can actually compute them quite accurately. These new techniques and the software packages that implement them still need their accuracies assessed (Remondino et al., 2012) which partially is the purpose of this paper.

In this study, the PC generation performance of three different software packages, referenced as Package 1, 2 & 3 in this paper, are tested to assess their accuracy, using Nikon D800 imagery acquired from an octocopter platform. GCPs were also surveyed to tie the model to a local coordinate system. To assess the accuracies of these models, the statistics of the error at GPCs were analyzed as well as a comparison of the PC models.

2. EQUIPMENT AND TEST FLIGHT

UAS flights were executed with a Bergen Octocopter with a fixed down-looking Nikon D800 camera equipped with a Nikon Nikkor AF-S 50mm f/1.4G lens (Figure 1). This full-frame camera takes high resolution images at about 36Mpix. The chosen lens was a good combination of field of view and small distortion which is usually the negative feature of lenses with short focal length. Additionally, the camera has its own GPS receiver which provides image geolocation tagging; however, this data as well as data from the octocopter MEMS IMU and dual-frequency GPS were not used in this investigation. Test flights were performed on January 14th, 2014 over three sites, all around the Olentangy River, Columbus, OH. The first site was taken over the Olentangy River Trail bike bridge at Broadmeadows Park. The second site was part of the Olentangy River close to the Whetstone Park. The third site also included a bike bridge on the trail, at the northwest end of Union Cemetery. These test sites were intentionally chosen because of the difficulty in modeling the bridges and the immediate area around the riverbank, which includes large amounts of canopy cover making it difficult to distinguish surfaces. All three missions were planned as an autonomous flight using DJI Ground Station Software. The combination of hardware features, such as FOV, flight duration, and flight purpose (mapping the bridge and both riverbanks) determined the project flight plan as two strips with flying height of 135 m (Site 1) and 125 m (Site 2 and 3) above ground level. The flying heights resulted in an estimated GSD of about 1.3 cm. The cruise speed chosen for all flights was 4 m/s and images were taken with the constant interval of 1 s. Settings of the project flight resulted in the final side- and endlap of more than 90%. This helped avoid any gaps caused by the instability of the rotor platform while improving the geometry of the final model.

Figure 1. OSU octocopter UAS at Site 3

Numerous GCPs were GPS-surveyed in the area to be used in model creation. Unfortunately, the landscape of Site 2 was so hard to model that it was too difficult to find enough points with sufficient natural characteristics that could be used as GCPs. The limitations in creating the model of Site 2 meant it was measured and modeled in a different way than the models of Sites 1 and 3, and was therefore left out of this analysis. Note that for Sites 1 and 3 there were problems finding well distributed GCPs in the difficult to model terrain. The location of GCPs was not optimal in terms of AT, though the large image overlap resulted in robust block adjustment. This allows for assessment of the software packages in difficult circumstances. Field surveys of GCPs were executed using the GPS-RTK technique resulting in the 3D accuracy of GCPs of slightly less than 5 cm.

3. SOFTWARE PACKAGES AND PROCESSES

The software packages used in this analysis are looked at as a black box for model creation. All three packages accepted the same data inputs and generally followed the same process with some difference in algorithms leading to differing degree of points, matching, and accuracy. Processing in all three packages, although treated as a black box form the algorithmic perspective, is divided into few consecutive stages that the user performed in order to generate a dense PC. Generally, the workflow in all three packages consists of two separate parts: images block adjustment and dense matching. Results of both processing parts were analyzed in this study as they provide similar parameters which help in assessing the accuracy of the final PC models.

4. MODEL ACCURACY ASSESSMENTS

To assess the accuracy of the models, we used two different approaches. The first approach is to analyze the statistics of the bundle adjustment, as it is the initial process, in three aspects. The first aspect is the accuracy of the individual measured GCPs within the model defined by residuals with respect to the GPS-surveyed coordinates of these points. The second aspect is the usage and number of TPs. The third aspect is the analysis of the estimated camera calibration parameters performed during bundle adjustment. The second approach is to analyze the dense PC generation. Analysis of dense matching was performed by relatively comparing the PCs to each other including statistical and visual examination as well as through ground check points residuals.

4.1 Block Adjustment

To assess the accuracy of the block adjustment performed by the packages, an error analysis of the GCPs was performed. First, the GCPs root-mean-squared-error (RMSE) was calculated to find the magnitude of varying quantity. This gives a good measure of the total difference or residuals between the predicted values of the location of the GCPs in the model and the observed values of the GCPs from GPS. In addition, the maximum residuals were also included to show that there were no outliers contained in data. The projection of pixel error is included as it shows the accuracy of the pixel within the images.

Looking at the number of tie points (TP) and projections (rays) used in AT shows the ability of each package's algorithms to find and match the same pixels and the strength of the bundle block adjustment.

Looking at the data for the camera self-calibration produced by each package allows us to see its accuracy of the built-in calibration techniques. Since the same camera is used for both test sites, each package should generally repeat the same camera internal parameter results. Packages 1 & 2 provide estimates on focal length and (x, y) location of the principal point, while Package 3 only provides focal length estimates. The initial parameters were also selected by each package so they were also slightly different. Since the camera was not calibrated in lab, it cannot be stated which is more reliable, but the packages should estimate the same parameters for both sites which was the circumstance assessing theirs accuracies.

4.2 Point Cloud

Comparing the PCs to each other can tell us the distances between points and whether there is a bias with regards to direction. Secondly, point spacing shows how dense the matching is, showing the performance of the each package.

Visual examination of the PCs also benefit with errors in the models being easily interrupted by the eye. It is possible to check the behavior of the algorithm in generating points for difficult objects like dense vegetation, small parts of the bridge structure, or the extremely challenging river surface.

Absolute accuracy of the PCs geometry can be assessed using GCPs which become ground check points since they are not used during dense matching and PC generation. Measuring coordinates of check points by selecting them manually in the PC and comparing their coordinates with the GPS-surveyed points treated as reference, can calculate absolute errors of the PC geometry. The error exhibited in the bundle block adjustment is expected to multiply in the second process of PC generation.

5. RESULTS

The models for the two sites were run with the same images and parameters that were able to be selected in each package. There were 16 GCPs and 51 images selected for Site 1, and 15 GCPs and 47 images selected for Site 3. The ground control error/tolerance was also set the same for all software packages, at 5 cm. The initial conditions being the same (as permitted by the packages) allows for only the comparison of the package and their algorithm implantation.

			Package 1					Package 2					Package 3			
			3D	X	Y	Z	Projection	**3D**	X	Y	Z	Projection	**3D**	X	Y	Z
			(cm)				(pix)	(cm)				(pix)	(cm)			
RMSE	Site	1	**3.6**	2.4	1.6	2.1	2.3	**6.0**	2.5	1.4	5.2	2.1	**7.1**	2.3	2.9	6.1
		3	**9.1**	6.4	3.7	5.4	2.4	**13.9**	4.9	4.4	12.3	2.8	**73.1**	20.7	19.0	67.4
Max	Site	1	**5.9**	4.9	4.2	4.0	6.8	**16.6**	6.6	3.0	16.3	3.4	**16.5**	5.6	6.0	16.4
		3	**17.2**	12.5	8.0	14.2	3.8	**32.9**	10.8	11.2	32.8	4.2	**190.3**	64.0	66.5	177.7

Table 1: Statistics of GCPs for bundle block adjustment.

		Package 1			Package 2			Package 3		
		Distance	Point *x*	Point *y*	Distance	Point *x*	Point *y*	Distance	Point *x*	Point *y*
Adjusted values	1	51.25	17.93	11.81	51.11	18.09	12.00	46.5 – 55.5	17.95*	11.98*
	3	51.68	17.94	11.82	51.51	17.95	12.01	47.2 – 56.7	17.95*	11.98*
Initial values		49.88	17.95	11.98	51.2	17.95	11.98	50	17.95*	11.98*

Table 2: Statistics of tie-points for bundle block adjustment

		Package 1			Package 2			Package 3		
		Distance	Point x	Point y	Distance	Point x	Point y	Distance	Point x	Point y
Adjusted values	1	51.25	17.93	11.81	51.11	18.09	12.00	46.5 – 55.5	17.95*	11.98*
	3	51.68	17.94	11.82	51.51	17.95	12.01	47.2 – 56.7	17.95*	11.98*
Initial values		49.88	17.95	11.98	51.2	17.95	11.98	50	17.95*	11.98*

Table 3: Statistics of camera parameters for bundle block adjustment. Note that package 3 does not adjust Principle point location.
* Not estimated (equal initial values)

5.1 Image Block Bundle Adjustment

Since all packages use a bundle block adjustment as a step of a PC generation, we decided to give some statistics telling about the accuracy of this process. Table 1 shows the statistics for the GCPs, reporting about the model georeferencing. Table 2 shows the statistics for TPs, analyzing the matching ability included in the bundle adjustment of each package. Table 3 shows the camera adjusted parameters since the camera self-calibration is included in the bundle adjustment algorithm of each package.

As seen in Table 1, Site 1 had remarkably low RMSE of 3.6 cm for Package 1, lower than the GCPs 3D tolerance level of 5 cm, meaning that the bundle adjustment met the assumed accuracy condition. In the case of Package 2, it had a 3D accuracy slightly larger; however, it is still on the level of GCPs error tolerance. Package 3 was still only slightly larger than that. The low 3D RMSE for all packages show that the GCPs while not ideal were distributed well enough for an accurate bundle adjustment to be done by all packages.

The RMSE for Site 3 was 2-3 times larger than for Site 1 and for Package 1 and 2. It was even larger for Package 3, about 10 times larger than for Site 1, with an error of 73.1cm. Site 3 having larger errors for all packages showed that the GCPs distribution for it was worse than for Site 1. Package 1 still performed well and had 3D error less than double the tolerance (10 cm), as it was our nominal goal. Package 2 performed slightly worse but was still able to perform a relatively accurate bundle adjustment although larger than our benchmark. Package 3's model error was massive and showed that it could not perform a good bundle adjustment with the poor set of GCPs.

Judging the results, we need to consider that test sites were selected to be somewhat difficult containing a river in the middle of dense canopy area. Thus, it challenged not only the image matching algorithms but also made the collection of optimal distributed GCPs difficult. With this recognition, this data shows that Package 1 was able to handle the less than ideal modeling scenes to produce the most accurate block adjustment. Package 2 also performed well, just above the tolerance in Site 1 and just above the goal of 10 cm in Site 3. Package 3 fared the worst in Site 1 although still below 10 cm and with large errors in Site 3

Table 1 also shows the coordinate residuals for the models. The residuals for all three axes were similar for Package 1 at both sites, meaning that the model was not biased in any direction. For Package 2 and 3, the Z-axis residuals were larger for both sites. This error was expected to be observed since the elevation estimates of the model are more difficult to accurately calculate. This is because the accuracy of space resection and intersection included in the AT process decreases with an increasing flying height. The first package having about even residuals in all components is impressive for the algorithm to create the model.

The maximum absolute residuals show that there were no gross outliers contained in the bundle adjustment which partially can prove the correctness of this process for each package.

Packages 1 and 2 Pixel Projection errors for both sites are similar and quite small considering the use of a non-metric camera, sites situated over the river and non-optimized distribution of the GCPs. Note that value of 2.5 pixels on digital image is equivalent to about 12 μm of the physical image dimension (considering 'full frame' size of the used image sensor).

The large number of correct TPs significantly strengthens the block geometry, but also extends the processing time. Table 2 shows that Package 1 was able to detect many more TPs than Package 2 which was still more efficient than Package 3. There is also no correlation seen between sites and number of TPs and projections. Considering the TP and projection error, it is clear that Package 3 is using the least efficient matching algorithm as not only the number of projections is the smallest, but also, it results in the largest error. Comparing accuracy of matching between the first two packages, Package 2 gives a very low projection error. This is probably explained by the threshold of matching. Package 1 may use lower requirements resulting in a larger number of TPs but also larger errors where Package 2 may remove these matches causing lower number of projections and lower error.

Discussing results in Table 3 of the camera calibration process it must be emphasized that the camera parameters were the same for each image taken over one site. The principal distance might be different for each site, since the focusing distance was set manually, and was slightly different for each site. In the case of Package 1, the difference in estimated position of the principal point between sites is insignificant which proves that parameters were estimated properly. The focal length was slightly larger than the initial for Package 1 but was about the same for both sites and near the estimated value, so it is assumed to not be an error. As seen in the calibration done for both sites by Package 2, the initial parameters were very close to the final parameters; however, the *x* position of the principal point is 0.14 mm different from the initial estimate, for Site 1. This offset may indicate error in the self-calibration process. In Package 3, the principal distance was estimated separately for each image clearly causing larger errors as the difference between estimated principal distances can differ by almost 10 mm. Secondly, in the Package 3, the principal point position is not estimated and the initial values are used which means the center of the image. Unfortunately, none of the packages show the accuracy of the estimated values making it difficult to assess the reliability of given parameters.

5.2 Point Clouds Statistics

Generated PCs are dependent on the used algorithm. Top view visualization of PCs for Site 1 and Site 3 are presented in Fig. 2 where the relative scale within one site is preserved. Statistics of the number of total points and point spacing calculated for the models are given in the Table 4. Note that due to matching failures, e.g. on the river surface/canopy, point spacing was calculated based only on the target model areas where algorithms should work properly, e.g. on the pavement.

	Number of generated points			Point spacing [mm]		
	Package 1	Package 2	Package 3	Package 1	Package 2	Package 3
Site 1	9983916	58457652	2071963	40	11	44
Site 3	8863044	40632909	1481862	32	10	33

Table 4. Statistics for generated point clouds

For Package 1, the area covered by points is the largest. For Package 2, every ground sample has an assigned point. For Package 3, the number of points is smallest and points on the water and the ground are missing (upper and lower part of Figure 4, b3). For Package 2, the area is smallest (strange automatic cuts to the area of interest), but the number of points, points density is the largest, and point spacing is even smaller than estimated GSD. Point spacing for Package 1 and 3 are similar and equal about 3-4 cm. Comparison of details mapped through different point density is shown in the Figure 2. Note that for visualization purposes, the thickness of points for each package is different due to different point spacing.

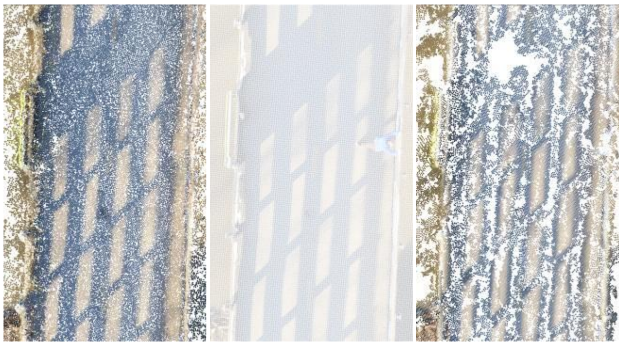

(a) (b) (c)

Figure 2. Visualization of details mapped by points for Site 3 and Package: (a) 1, (b) 2, (c) 3

There are visible difficulties in matching for Package 3, especially in shaded, dark areas. Package 2 uses an algorithm which finds (computes) a point for every pixel, even if it is not always the best solution, since the computed matches might be wrong.

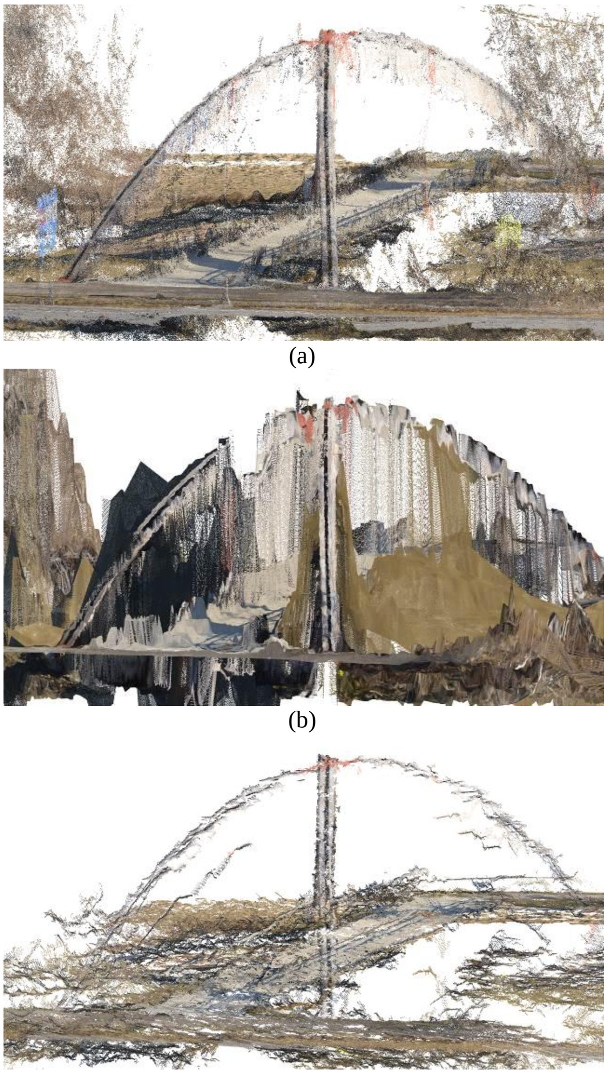

(a)

(b)

(c)

Figure 3. Isometric view on the point cloud of the bridge obtained using Package: (a) 1, (b) 2, (c) 3

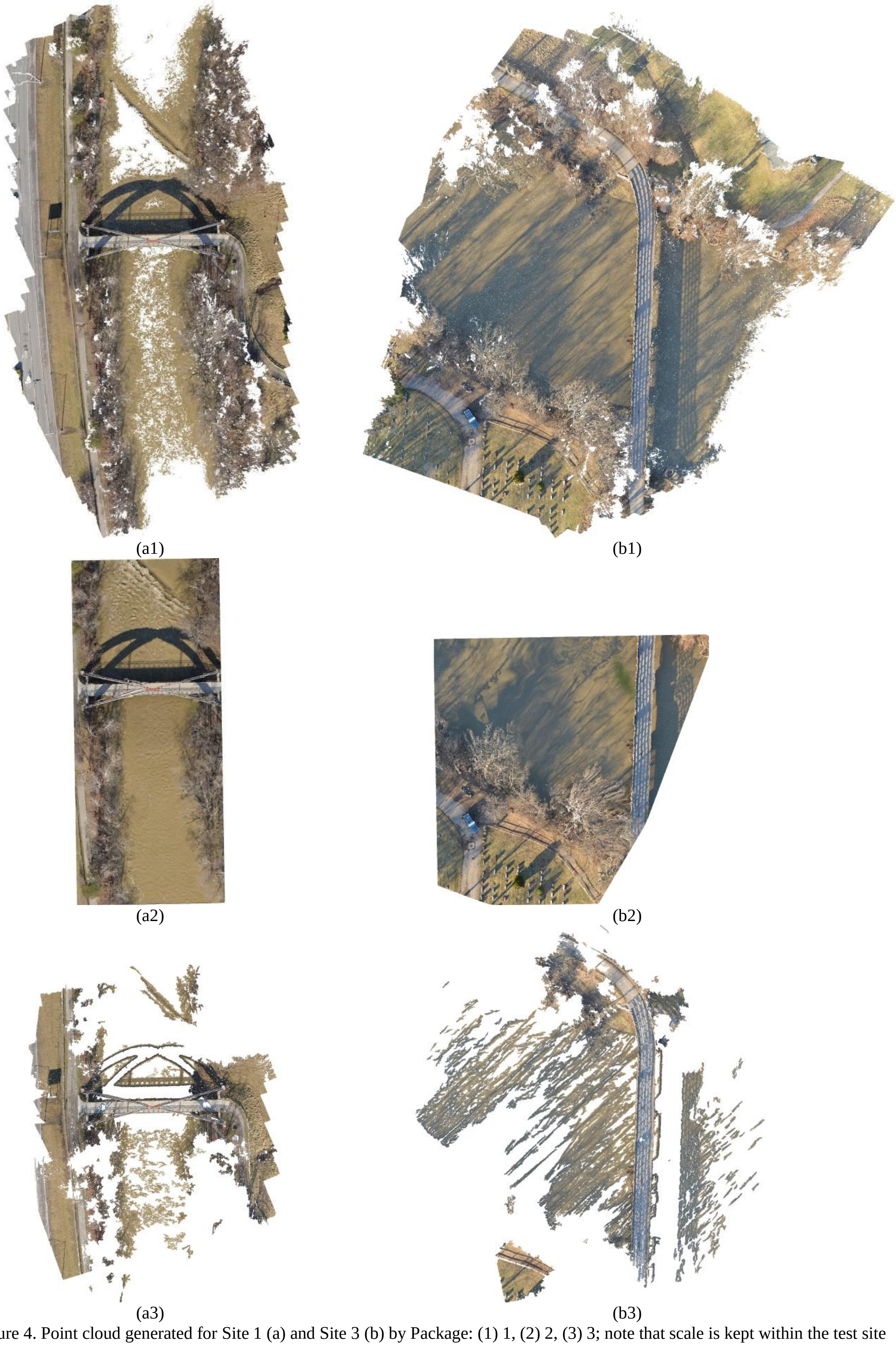

Figure 4. Point cloud generated for Site 1 (a) and Site 3 (b) by Package: (1) 1, (2) 2, (3) 3; note that scale is kept within the test site

			Package 1					Package 2					Package 3				
			3D	X	Y	Z	No. of check points	3D	X	Y	Z	No. of check points	3D	X	Y	Z	No. of check points
			(cm)					(cm)					(cm)				
RMSE	Site	1	12.1	5.9	7.4	7.6	28	16.2	7.9	4.2	13.5	11	26.7	7.3	6.6	24.8	26
		3	8.6	4.6	4.4	5.8	15	13.4	3.3	5.6	11.7	6	51.7	8	9.2	50.2	12
Max	Site	1	21.6	16.2	16.5	20	28	32.8	17.2	77	32.3	11	95.2	21.2	19.1	94.8	26
		3	14.7	9.3	10.1	11.2	15	28.8	6.7	11.5	26.4	6	89.2	16.2	17	87.5	12

Table 5: Point clouds absolute accuracy.

As shown in the Figure 3, the number of wrongly matched points for Package 2 is the largest. There are not only interpolation errors, e.g. between the bridge pavement and frame (arcs), but also a lot of other points (not just on the river and canopy area) where the designated elevation is much higher or lower than the actual surface. In this case, an automatic filtering would probably fail in DSM, DTM, or object point extraction. For Package 3, the number of points is smaller and without significant errors. The visible pavement surfaces are not smooth as they should be. Package 1 shows the reasonable balance between numbers of correctly and wrongly matched points. There are small errors (e.g. on the top of the bridge frame) or points on the water (not all matched wrongly) which should be easily eliminated in the subsequent post processing. For this package, even points of small elements as railing on the bridge are correctly kept.

Accuracy of generated PCs can be evaluated in the absolute sense, i.e. using ground check points. Results of this evaluation are presented in the Table 5.

Interpreting results from the Table 5, it must be emphasized that points in the PCs were selected manually based mainly on colors as most of the check points were placed on the flat surfaces (all in the case of Site 3). The number of check points for each package was different for the same site, as not all points could be recognized and selected. For Site 1, part of check points were placed on the corners and edges which can explain much larger errors than for Site 3 (except in Package 3 where block adjustment was so poor). The given values beside bundle adjustment errors contain interpretation errors and are affected by the PC density.

The same trends witnessed in Table 1, for the GCPs are exacerbated for the check points. This was expected as the error of selecting them is also added to the error of the GCPs. Package 1 still exhibits no bias on the z axis and the other two packages do. Both Package 1 and Package 2 have errors within acceptable ranges when including the added error, for Sites 1 & 3. Package 3 still has the largest error and is outside of the acceptable error range for both sites.

Another way of validating results might be the relative comparison of PCs, using CloudCompare (Girardeau-Montaut, 2014). This allows us to see the distances between points and the variation of the measurements. For this, we compared only the bridge section of each site. This was done so the most accurate portion and target area was compared and no large errors from the unmatchable canopy and water surface areas of the models were included in the comparison. In this comparison, the most densely populated PC was set as the reference. This was done to lower the error created from comparing against a sparse PC since distances are calculated for every point in the compared cloud. As shown in Table 6, Package 2 was used as the reference package for the comparison between it and Packages 1 and 3. Package 1 was used as the reference when comparing to Package 3.

In the distance comparison, Package 1 and 2 were close to having their models match. This shows that these packages' PCs were very similar even with the compounding errors from bundle adjustment and PC generation in the well modeled bridge area. The comparison between Package 2 and 3 as expected from the GCP statistics was larger. While both packages modeled the area well, the offset between the whole PC compared to each other was large. This was due to large bundle adjustment errors for Package 3 causing the bridge area to also be offset. The comparison of Package 1 to 3 was also large as was expected from the previous comparison.

Reference Package to Compared		Site 1	Site 3
2 to 1	3D Mean Distance [cm]	3.1	1.7
	Standard Deviation [cm]	2.9	1.6
2 to 3	3D Mean Distance [cm]	6.9	17.3
	Standard Deviation [cm]	7.5	14.7
1 to 3	3D Mean Distance [cm]	9.4	17
	Standard Deviation [cm]	11.1	14.2

Table 6. Cloud comparison distance and standard deviation of a well modeled area for all packages

The cloud to cloud comparisons for the PCs showed similar trends from the previous GCP analysis. Packages 1 and 2 were similar in the well modelled areas. Site 3 distances being smaller than Site 1 in Packages 1 and 2 was unexpected yet both errors were small enough to negate the difference from the GCP analysis and can be attributed to the smaller sample area. Package 3 had a larger distance when comparing as seen with the GCP comparison. While Package 1 had the best bundle block adjustment, its comparison to Package 3 was worse than Package 2's comparison to Package 3. This is probably due to the elevation (Z-axis) bias found in both Packages 2 and 3. The larger elevation bias in Package 3, made its PC comparison distance further to Package 1, than 2.

6. CONCLUSION

The models created by images from a UAS can be processed with a variety of UAS specific software tools. Using field data from a practically hard to model area, we were able to show the benefits and deficiencies of three different software packages. Overall, Package 1 returned the best results when looking at both bundle block adjustment results and the generated PC models for both sites. Package 2 was also effective and created accurate models just not as well as Package 1. Package 3 returned the least accurate models. All three packages showed that the accuracies of models created with less than ideal data and landscapes can be close to, if not within, the error tolerances of the GPS used to collect the GCPs.

It is important to remember that this data set is difficult to model and with other data sets the results could change. The poor distribution of GCP at both sites could have contributed greatly to the amount of error seen. User deficiency in GCP selection and actual measurements are also variables that may have contributed to the error. With more data collection and field tests, comparison of the image models to each other and with models from LiDAR and laser scanners can be performed to allow for a differing analysis of the packages to help find which package and process is the most accurate and appropriate to use. UAS uses are vast and allow for the collection of survey grade spatial data and whose data and products must still be verified and studied with reports like this.

REFERENCES

Gini, R., D. Pagliari, D. Passoni, L. Pinto, G. Sona, and P. Dosso, 2013. Uav Photogrammetry: Block Triangulation Comparisons. *The International Archives of the Photogrammetry, Remote Sensing and Spatial Information Sciences,* Vol. XL-1/W2, pp. 157-62.

Girardeau-Montaut, D. 2014. CloudCompare - Open Source Project. *http://www.danielgm.net/cc/* (accessed 09 June 2014.

Haubeck, K., and T. Prinz, 2013. A UAV-Based Low-Cost Stereo Camera System for Archaeological Surveys - Experiences from Doliche (Turkey). *The International Archives of the Photogrammetry, Remote Sensing and Spatial Information Sciences,* Vol. XL-1/W2 (2013), pp. 195-200.

Mikhail, E. M., Bethel J. S., and J. C. McGlone, 2001. Introduction to Modern Photogrammetry. New York: Wiley.

Niethammer, U., Rothmund, S., Schwaderer, U., Zeman, J., and M. Joswig, 2011. Open Source Image-Processing Tools For Low-Cost Uav-Based Landslide Investigations. *The International Archives of the Photogrammetry, Remote Sensing and Spatial Information Sciences,* Vol. XXXVIII-1/C22 (2011), pp. 161-66.

Remondino, F., Del Pizzo, S., Kersten, T., and S. Troisi, 2012. Low-cost and open-source solutions for automated image orientation – A critical overview. *Proceedings EuroMed 2012 Conference*, LNCS 7616, pp. 40-54.